Chapter 4

Measurement

This chapter presents the measurement of the fabricated integrated device using SOI substrates and SU-8 photoresist. SU-8 material characterization, SU-8 stress induced beams, and the fabricated 135°-flipped mirror integrated with photo diodes are discussed.

4-1 SU-8 residual stress

The residual stress in SU-8 was first characterized by measuring the warp of Si substrates. SU-8 was coated using the process in Sec. 2-2-1 and hard baked at 190°C. Figure 4-1 shows the measured surface profile of four silicon wafers for various hard bake time by an ET-4000surface profilometer. Figures 4-1 (a), (c), (e), (g) show the warp of the wafer before SU-8 coating; Figures 4-1 (b), (d), (f), (h) show warp after SU-8 coating and hard baked for 0min ,10min, 20 min, and 30min, respectively. Using Young's modulus E= 4.6GPa [31, 32] and measured film thickness of 21um, one can calculate the residual stress from Equations 2-7 and 2-8. As can be seen from the calculated residual stress in Figure 4-2, longer hard bake time results in larger residual stress. However, the stress becomes stabilized for bake time longer than 20min. The calculated stress value of 27MPa is used in Sec. 2-2-4 to analyze and design the stress beam. This value is close to the reported in Ref [34].

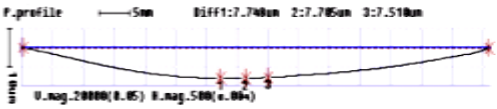

(a) bare wafer #1

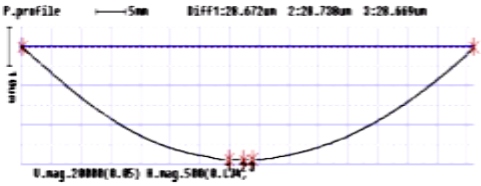

(b) SU-8 coated and hard baked for 0min.

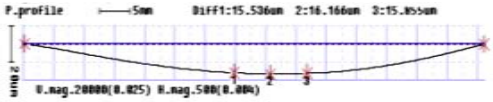

(c) bare wafer #2

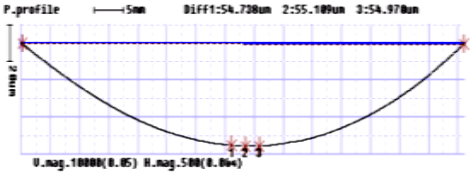

(d) SU-8 coated and hard baked for 10min.

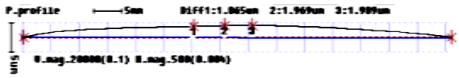

(e) bare wafer #3

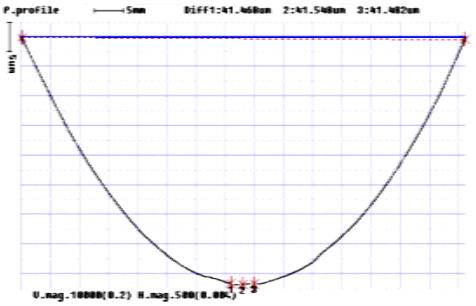

(f) SU-8 coated and hard baked for 20min.

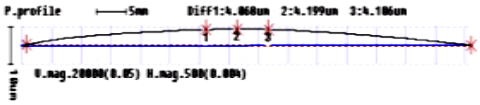

(g) bare wafer #4

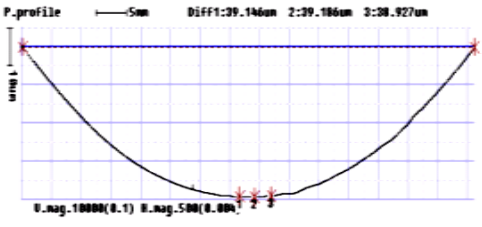

(h) SU-8 coated and hard baked for 20min.

Figure 4-1: Wafer warp due to SU-8 residual stress.

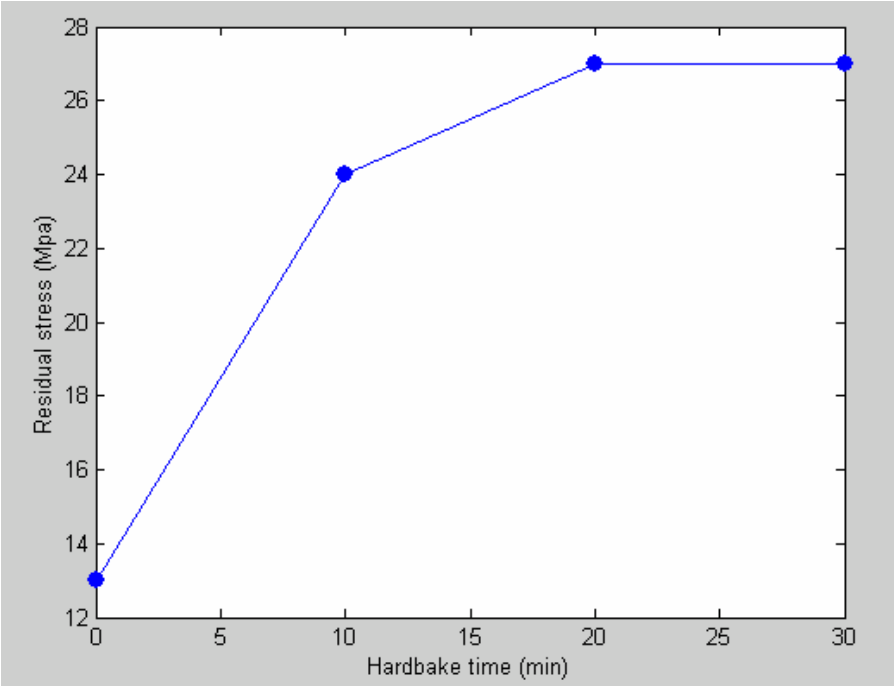

Figure 4-2: SU-8 residual stress vs. hardbake time.

4-2 SU-8 stress-induced beams

Figure 4-3 shows a released device where the stress beams are used to lift up and prevent the micromirror from sticking to the substrate. The vertical space under the lifted mirror also allows the use of probes to assemble the 135° structures.

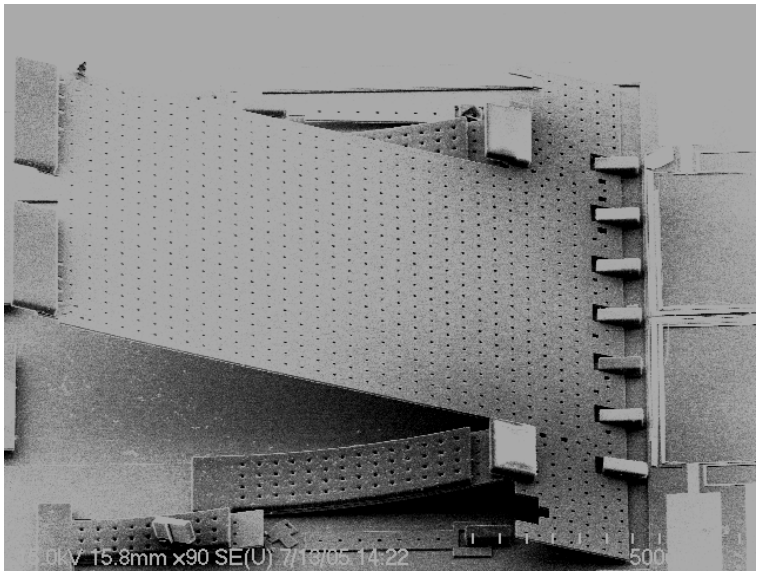

(a)

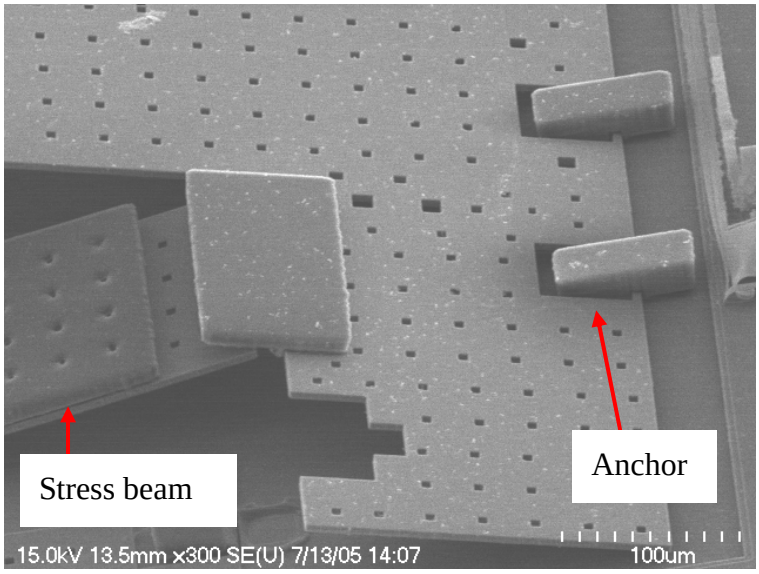

(b)

Figure 4-3: (a) stress beam lift up the micromirror after releasing (b) close up view.

Figure 4-4 shows the SU-8 stress-induced beams. Figure 4-5 shows the measurement of the longest stress beam in Figure 4-4. Figure 4-6 shows beam deflection of three beams with different length. The vertical displacement of the longest beam is about 26.2um. Compared with simulation in Sec. 2-2-4, the error is about 11%.

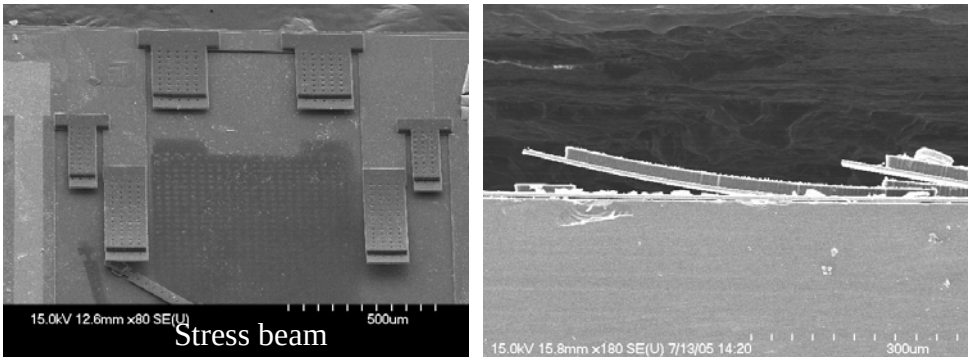

Figure 4-4: (a) SU-8 stress-induced beams. (b) cross section view.

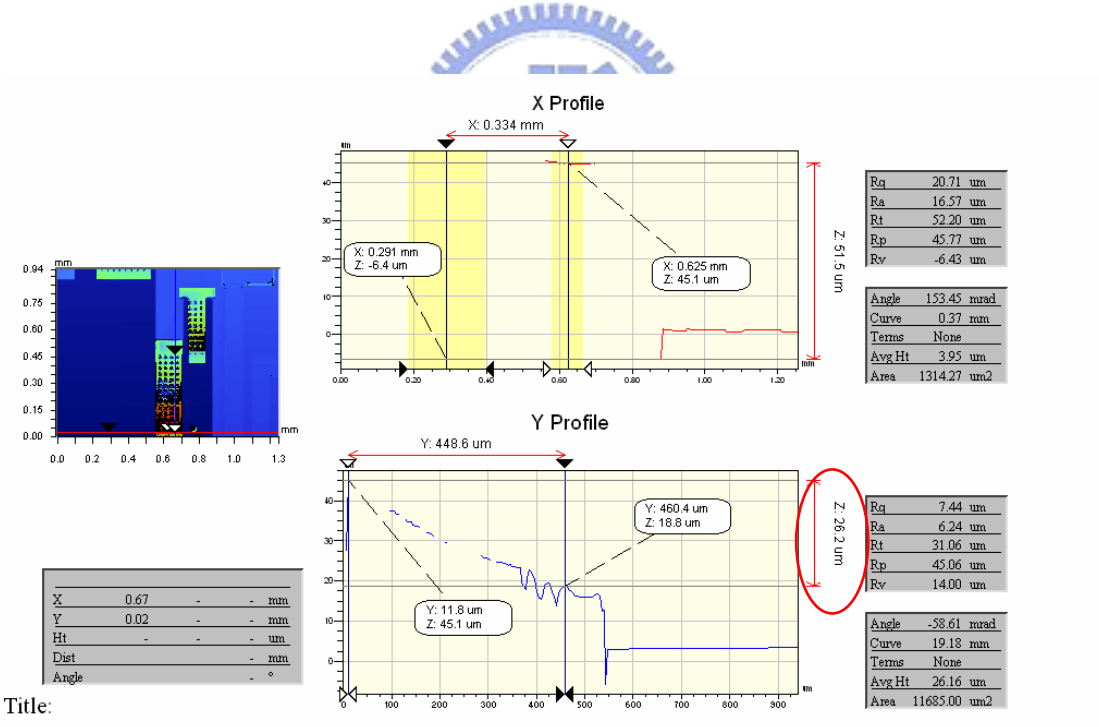

Figure 4-5: SU-8 stress-induced beam measured by a WYKO-NT1100 interferometer.

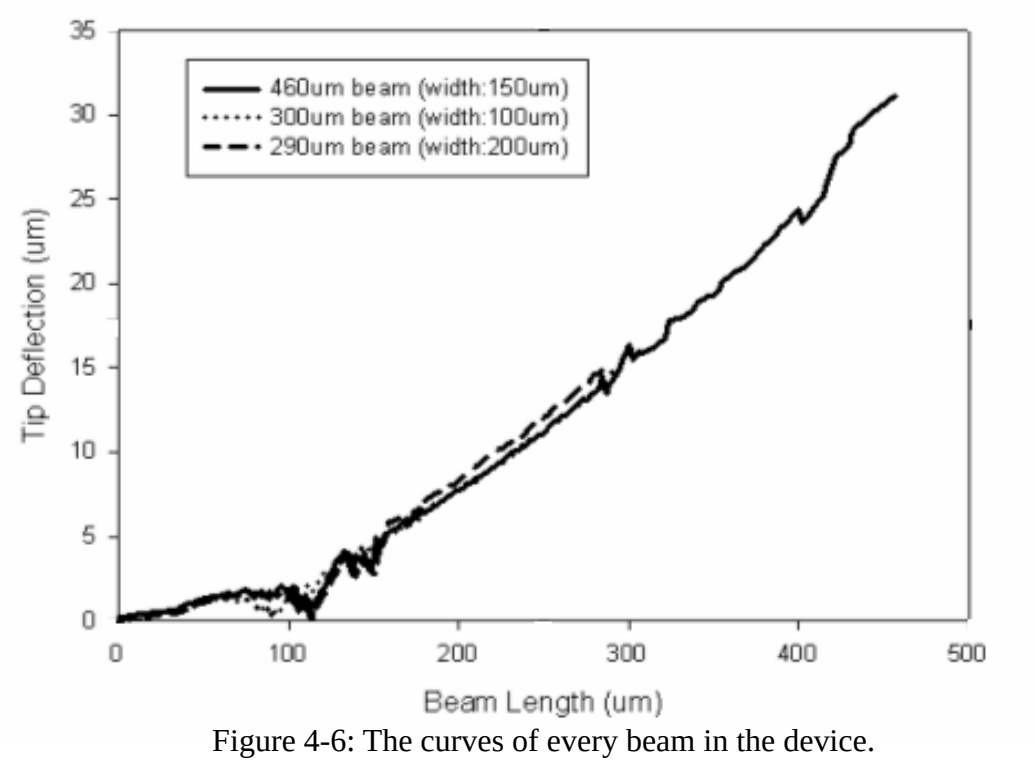

Figure 4-6: The curves of every beam in the device.

- **SU-8 aging**

The longer life time of stress beams are more useful for the positioning of the lifted components [14]. Therefore, aging of the stress beams are important. The relaxation of stress beams were measured for Au/polysilicon [16] and Si_xN_y/polysilicon [34]. Figure 4-7 shows the relaxation of the SU-8/SCS beams. The residual stress dose not show significant relaxation over a period of more than one month, as can be seen in the measured tip deflection in Figure 4-7.

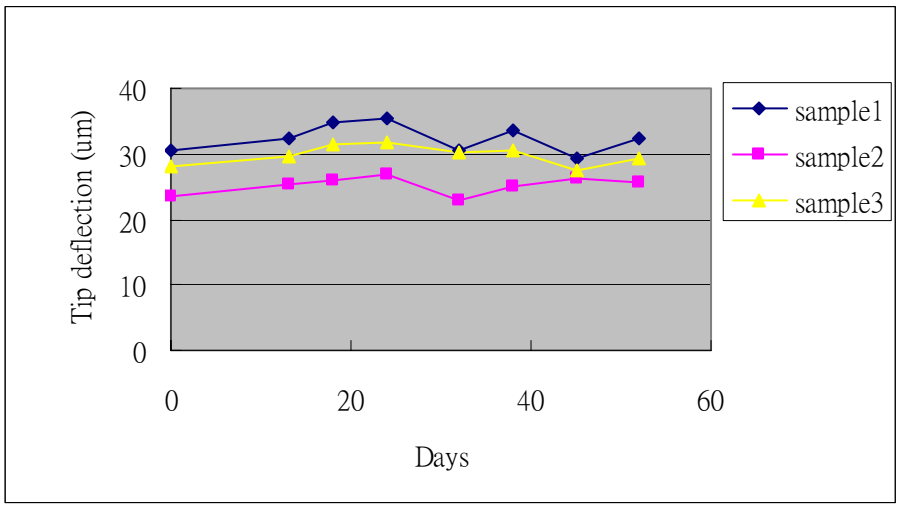

Figure 4-7: SU-8 aging.

4-3 Integrated Device with a 135°-flipped mirror and photo diodes

Figure 4-8 shows a 135°-flipped mirror integrated with photo diodes before release. The metal layer is clearly patterned. However, the metal layer peeled off, as shown in Figure 4-9. The micromirror was lost, too.

The metal peel-off problem can be attributed to the native oxide exiting on the silicon surface before the metal deposition. This can be solved by performing an HF dip before the deposition. The loss of the mirror is due to the small contact area of the SU-8 anchors, as discussed in Sec. 3-2-2.

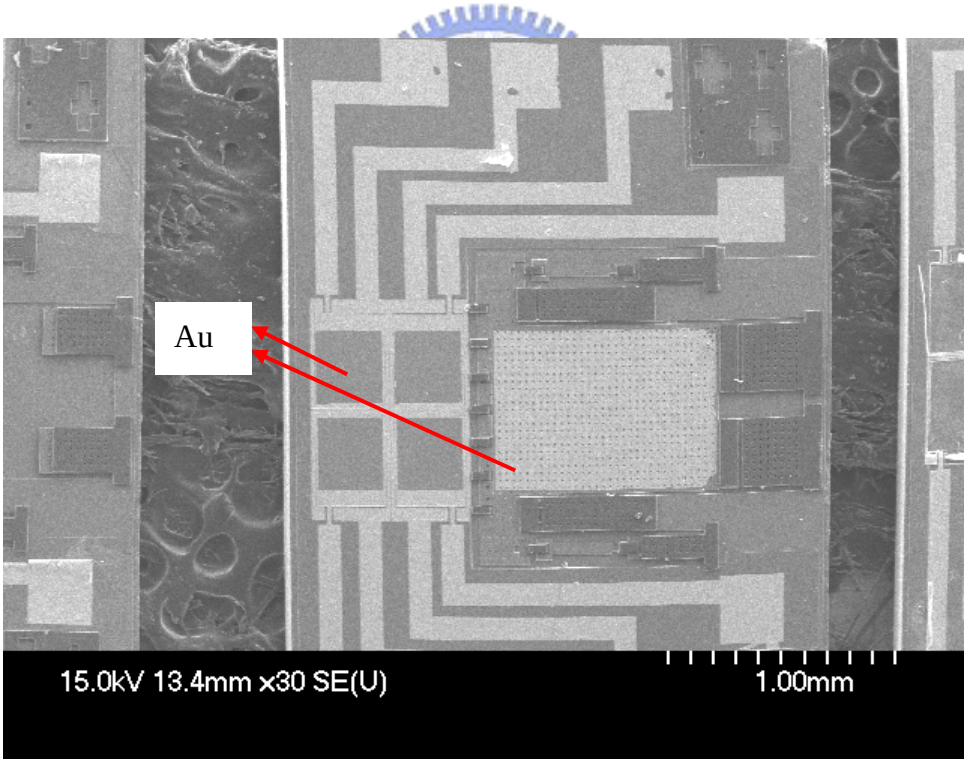

Figure 4-8: 135°-flipped mirror integrated with photo diodes before releasing.

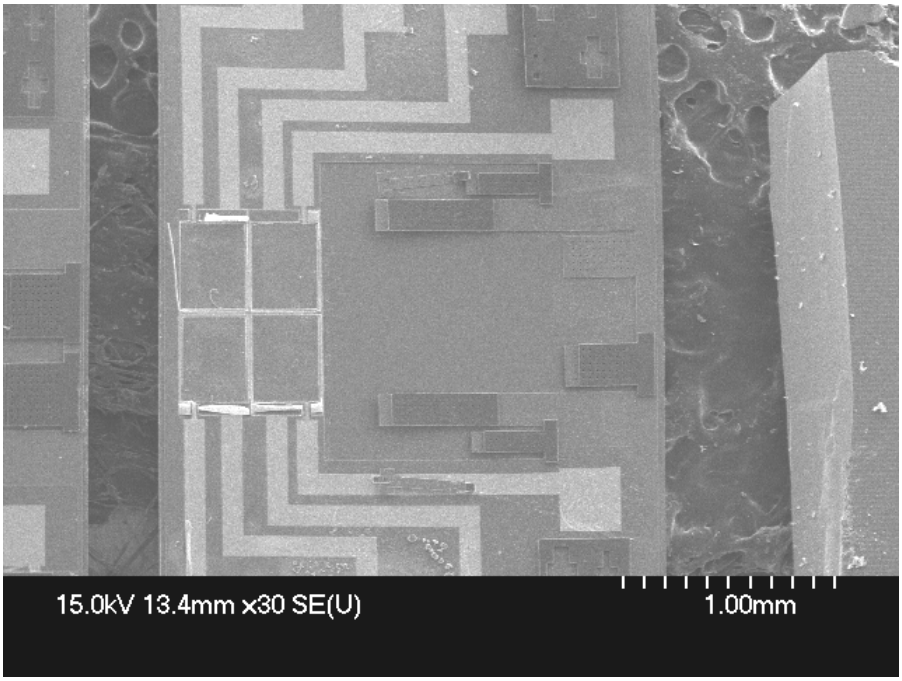

Figure 4-9: 135°-flipped mirror integrated with photo diodes after releasing.

Figure 4-10 shows a micromirror released using 49% HF vapor instead of direct immerging in 49% HF solution. This release process reduces the effect of surface tension of wafer so the device can survive more easily. However, the angle of the micromirror is quite different from the desired value (135°). It seems to be locked at a certain angle because of the gap of the anchors discussed in Sec. 3-2-2.

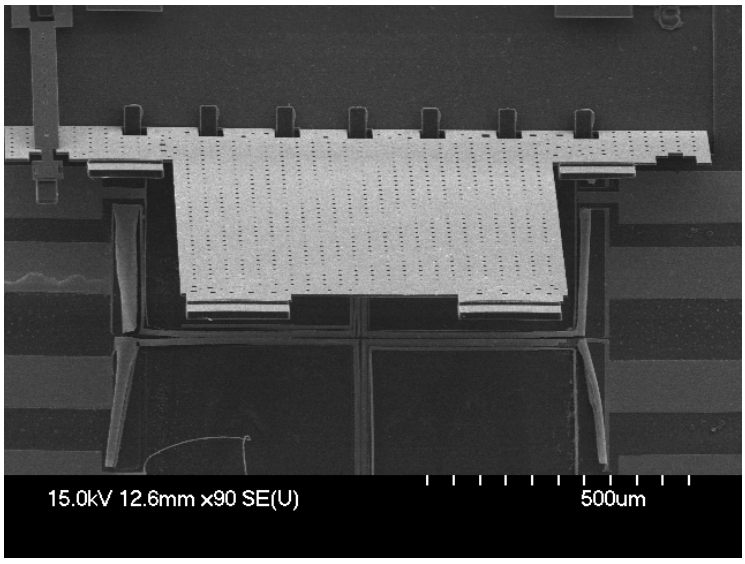

Figure 4-10: Top view of the device.

Figure 4-11 is the cross section view of a 135°-flipped mirror. The angle of the device is closer to 135° but it was also locked by the hinge bar sliding into the gap of the anchor.

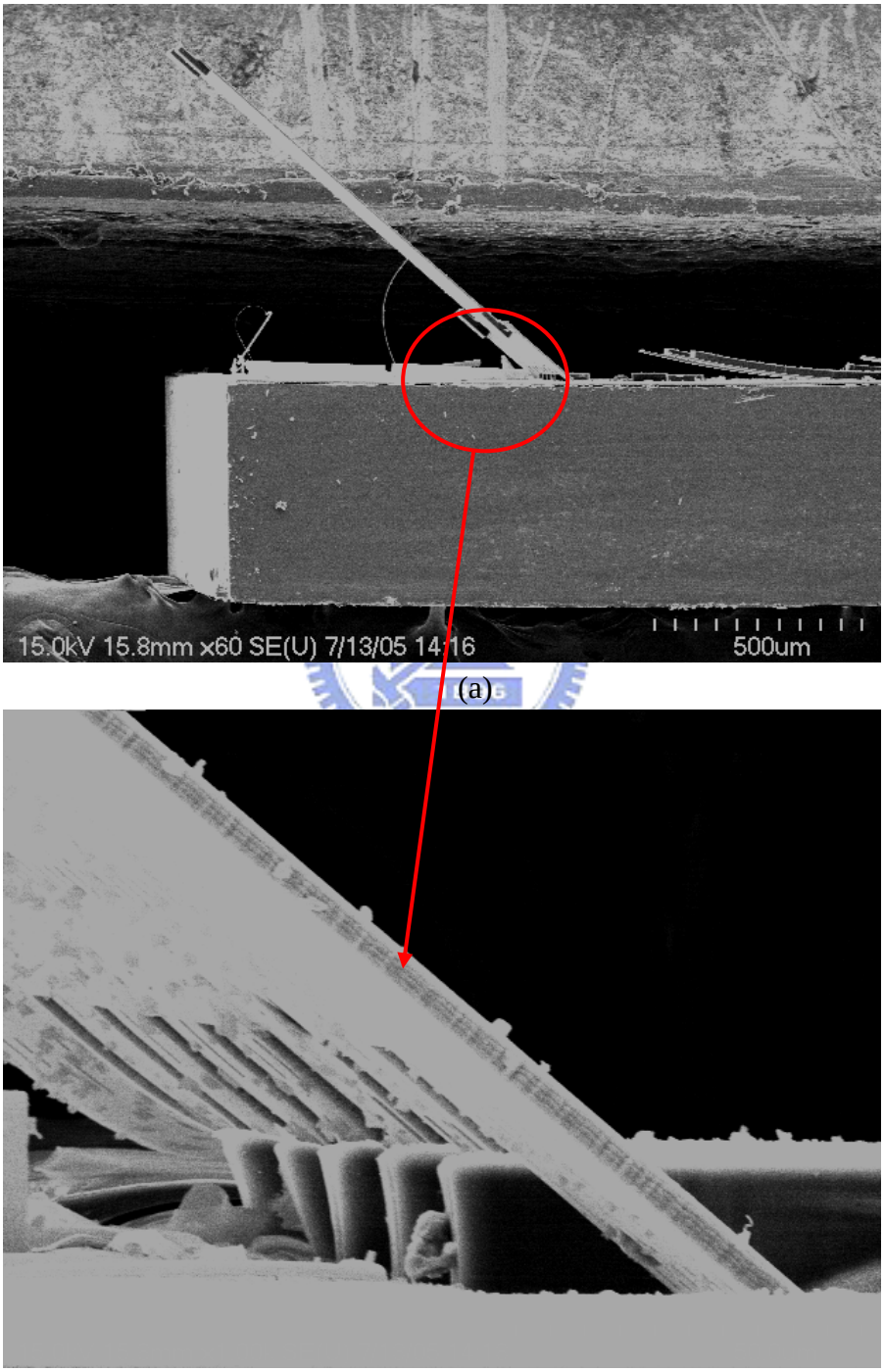

(a)

(b)

Figure 4-11: (a) 135°-flipped mirror without latch (b) close up view of the hinge and the micromirror.

Figure 4-12 is a 135°-flipped mirror locked by the latch. The angel of the micromirror is 150°, measured by a protractor. The angel is over 135° because the latch did not slide into the notch completely.

- **Photodector**

Figure 4-13 shows the quad photodectors for detecting the returned optical signal. The photodector was measured by Keithley 4200 semiconductor analyzer system before release. Figure 4-14 shows the I-V curves of one of photodiode with and without light. Figure 4-15 shows the detailed forward biased I-V curves. The solid line was measured without any light. The dashed line was measured with light illumination from the optical microscope. The power of the optical microscope light is 0.44mW measured by a Newport powermeter set at 650nm. The dimension of one diode is 94400 um^2 and illuminated area is 1.256×10^7 um^2. Therefore, the sensitivity can be calculated to be about 1.8 A/W.

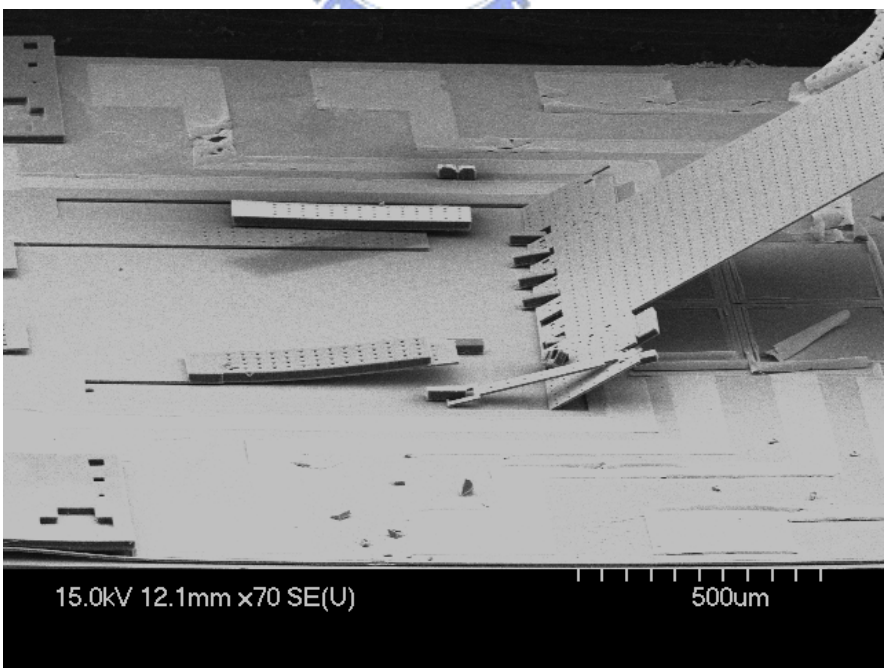

(a)

Figure 4-12: (a) 135°-flipped mirror with latch (b) cross section view of (a).

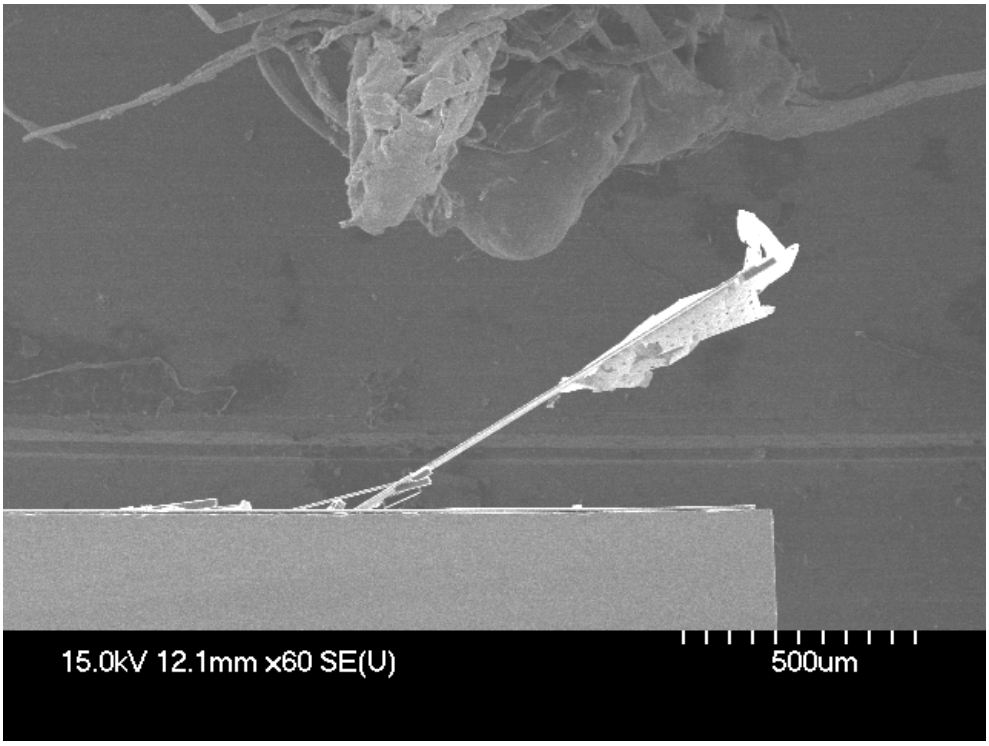

(b)

Figure 4-12: (a) 135°-flipped mirror with latch (b) cross section view of (a).

(Continued)

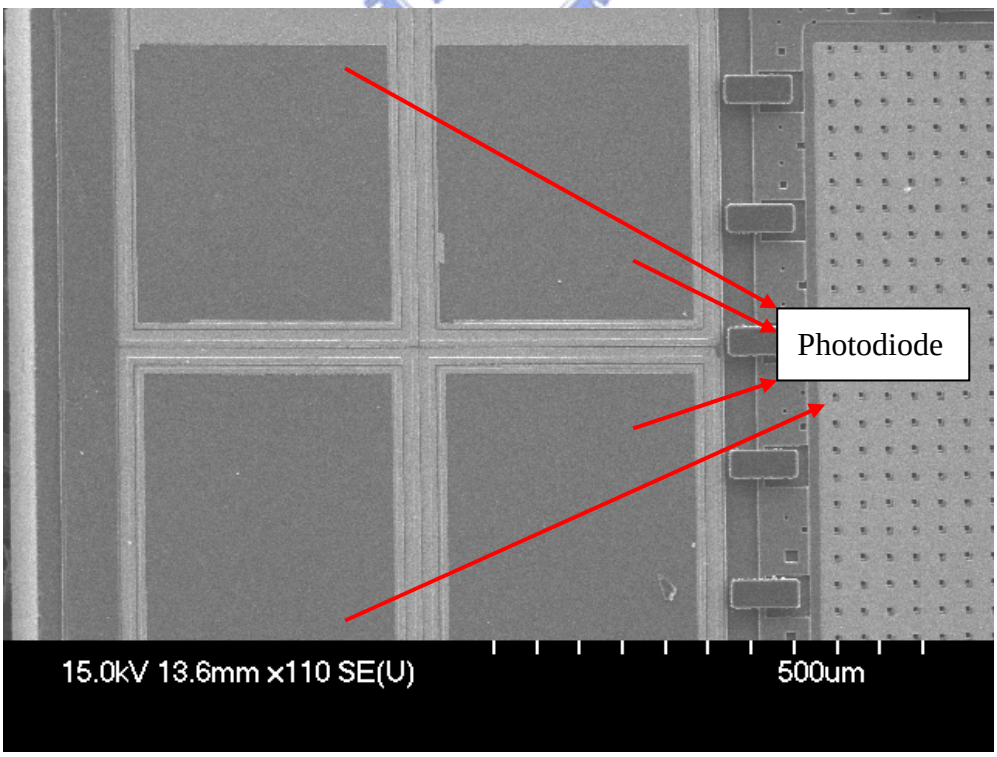

Figure 4-13: SEM of photodectors.

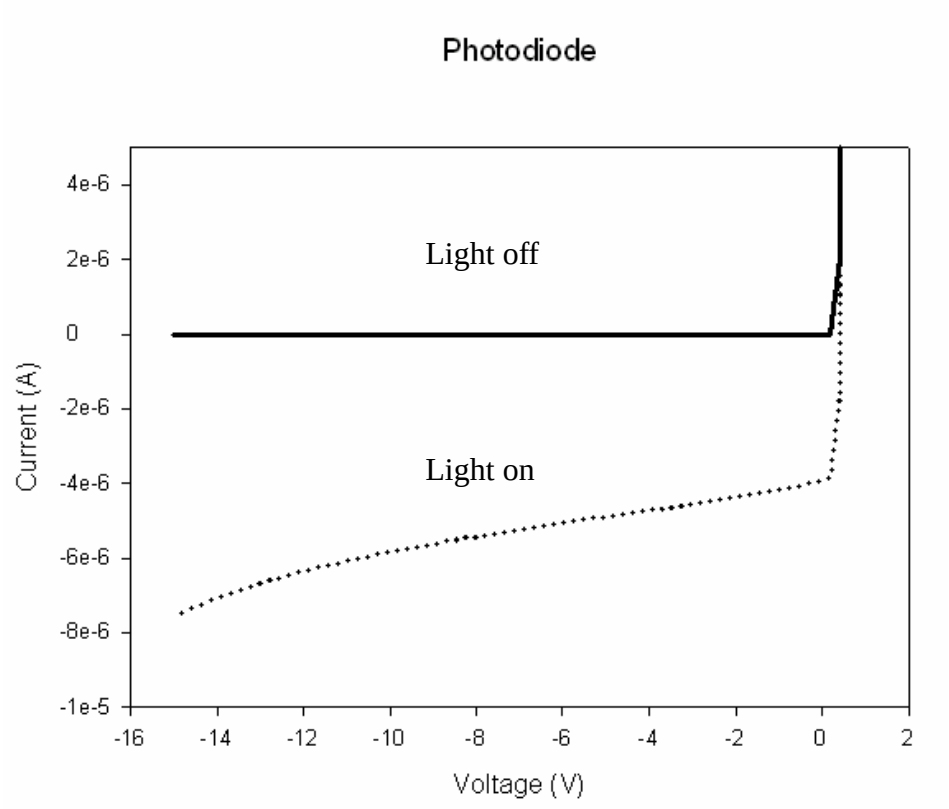

Figure 4-14: I-V curve of the photodiode with and without light.

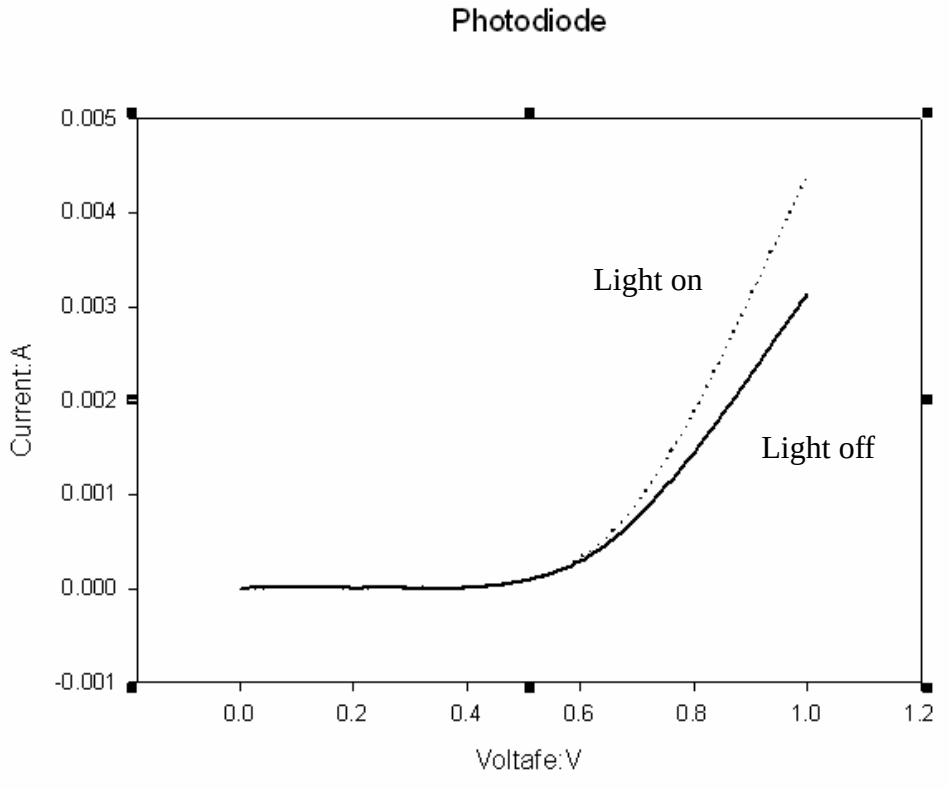

Figure 4-15: Forward biased I-V curves.